

SiO<sub>2</sub> and MgO compared to Al<sub>2</sub>O<sub>3</sub> and Fe<sub>2</sub>O<sub>3</sub>. Zoning of the pyroxenes is not observed and is unlikely to be preserved since intracrystalline diffusion is much more effective at high temperatures.

The preservation of an intrusive contact is therefore more consistent with models of the Neyriz ophiolite, that suggest an origin during continental rifting (20) (perhaps resulting in an ocean similar to the present-day Red Sea) rather than at the spreading center of a wide ocean destroyed through subduction (5) or partially obducted as a hot slab (4). Other ophiolites of the Tethyan belt, where evidence for subduction and obduction is often weak, may have originated in a similar manner.

ROBERT HALL

Department of Geological Sciences  
Queen Mary College, University of  
London, London E1 4NS, England

#### References and Notes

1. L.-E. Ricou, *Bull. Soc. Geol. Fr.* **13**, 146 (1971).
2. K. W. Gray, *Q. J. Geol. Soc. London* **105**, 189 (1949).
3. A. J. Wells, *Geol. Mag.* **106**, 385 (1969).
4. N. H. Woodcock and A. H. F. Robertson, *Geology* **5**, 373 (1977).
5. S. J. Haynes and H. McQuillan, *Geol. Soc. Am. Bull.* **85**, 739 (1974).
6. Pyroxene end-members have been calculated in the order suggested by H. S. Yoder and C. E. Tilley [*J. Petrol.* **3**, 342 (1962)]. Sodium has been assigned to acmite (NaFe<sup>3+</sup>Si<sub>2</sub>O<sub>6</sub>), and Tschermak's molecule (Ts) has been calculated as three end-members, aluminum Ts (AlTs, CaAl<sub>2</sub>Si<sub>2</sub>O<sub>6</sub>), ferric Ts (FeTs, CaFe<sup>3+</sup>AlSi<sub>2</sub>O<sub>6</sub>), and titanium Ts (TiTs, CaTiAl<sub>2</sub>O<sub>6</sub>).
7. W. A. Deer, R. A. Howie, J. Zussman, *Rock-Forming Minerals* (Longmans, London, 1978); C. E. Tilley, *Geol. Mag.* **75**, 81 (1938).
8. A. Knopf and D. E. Lee, *Am. Mineral.* **42**, 73 (1957).
9. H. G. Huckenholz, W. Lindhuber, J. Springer, *Neues Jahrb. Mineral. Abh.* **121**, 160 (1974).
10. H. C. Helgeson, J. M. Delany, H. W. Nesbitt, D. K. Bird, *Am. J. Sci.* **278A**, 1 (1978).
11. Experimentally determined equilibria are as follows: (i) calcite + quartz = wollastonite + CO<sub>2</sub> [H. J. Greenwood, *Am. Mineral.* **52**, 1669 (1967)]; (ii) calcite + anorthite + wollastonite = grossular + CO<sub>2</sub> [T. M. Gordon and H. J. Greenwood, *ibid.* **56**, 1674 (1971)]; (iii) anorthite + 2 wollastonite = grossular + quartz [A. L. Boettcher, *J. Petrol.* **11**, 337 (1970)]; (iv) grossular<sub>50</sub>andradite<sub>50</sub> = FeTs + 2 wollastonite (9). The position of the invariant point I (Fig. 1) has been taken as 600°C and X<sub>CO<sub>2</sub></sub> = 0.15. The positions of other equilibria have been calculated from data in (10). The effect of other components has been estimated: for garnet, by assuming an ideal solution model [J. Ganguly, *Contrib. Mineral. Petrol.* **55**, 81 (1976)]; for fassaite, by assuming that AlTs activity = X<sub>AlTs</sub>, which is consistent with experimentally determined activity-composition relations for Di-Hd-AlTs (Di is diopside, and Hd is hedenbergite) solid solutions with X<sub>AlTs</sub> < 0.3 [B. J. Wood, *Am. Mineral.* **61**, 599 (1976)] and assuming that FeTs activity = X<sub>FeTs</sub>. The activities of plagioclase, wollastonite, and calcite have been taken as unity.
12. B. M. Reinhardt, *Schweiz. Mineral. Petrogr. Mitt.* **49**, 1 (1969).
13. Complex inclusions ranging in size from a few microns to ≈ 20 μ are common in the pyroxenes as planar groupings traversing the host crystal but do not continue into the adjacent wollastonite, and they are therefore classed as pseudo-secondary inclusions. Similar, but isolated, inclusions occur and are interpreted as primary. The inclusions commonly contain more than 50 percent crystalline material and a low-density vapor phase which rarely has a rim of liquid. Some of the crystalline material appears to be calcite. Similar, though less common, inclusions occur in wollastonite. All these inclusions are interpreted as magmatic inclusions, an indication

that fassaite and wollastonite crystallized from a melt.

14. J. A. Willems and J. J. Bensch, *Trans. Geol. Soc. S. Afr.* **67**, 1 (1964).
15. R. J. Shedlock and E. J. Essene, *J. Petrol.* **20**, 71 (1979).
16. R. G. Coleman, *Bull. U.S. Geol. Surv.* **1247** (1967).
17. ———, *Ophiolites: Ancient Oceanic Lithosphere* (Springer Verlag, Berlin, 1977); H. Williams and W. R. Smyth, *Am. J. Sci.* **273**, 594 (1973); J. Zimmerman, *Geol. Soc. Am. Mem.* **132** (1972), p. 225.
18. R. Joesten, *Geol. Soc. Am. Bull.* **88**, 1515 (1977).
19. N. L. Bowen, *The Evolution of the Igneous*

*Rocks* (Princeton Univ. Press, Princeton, N.J., 1928); D. H. Watkinson and P. J. Wyllie, *Geol. Soc. Am. Bull.* **80**, 1565 (1969).

20. R. Stoneley, *Tectonophysics* **25**, 303 (1975).
21. I thank M. Arvin for the opportunity to visit Neyriz and H. S. Edgell for help with fieldwork. I thank P. Suddaby, N. Wilkinson, and K. Brodie, who provided assistance with microprobe analyses carried out in the Geology Department, Imperial College, London. I thank A. H. Rankin for examination and interpretation of the fluid inclusions and M. G. Audley-Charles and W. J. French for discussions.

3 December 1979; revised 14 March 1980

## Aragonite Twinning in the Molluscan Bivalve Hinge Ligament

**Abstract.** *Molluscan bivalve hinge ligaments are composed of long needle-shaped aragonite crystals embedded in a protein matrix. These crystals are twinned and, in general, the twin forms a thin lamella through the center of the crystal.*

By electron microscopy and electron diffraction of single crystals in thin sections, we have demonstrated that the aragonite (CaCO<sub>3</sub>) crystals in the molluscan bivalve hinge ligament are twinned. Aragonite is orthorhombic belonging to space group *Pmcn*. Inorganic sources of the mineral are commonly observed to be twinned about the (110) morphologic plane (1). Thin twin lamellae have been observed in electron micrographs of aragonite crystals from limestone deposits (2). Our experiments are apparently the first demonstration of twinning in biogenic aragonite, although Mutvei (3) has proposed that, on the basis of crystal morphology alone, the aragonite crystals of bivalve shell nacre are twinned.

The bivalve hinge ligament is composed of long needle-shaped aragonite crystals embedded in an elastic, predominantly protein matrix (4). The crystals are pseudohexagonal in cross section (Fig. 1), and the morphologically long (crystallographic *c*) axis is oriented perpendicular to the growing margin of the ligament. The crystals are about 100 nm in cross section. For electron micro-

scopy, 0.5-mm slices of the ligament were fixed in 5 percent glutaraldehyde in 0.1M cacodylate buffer, pH 7.6, for 4 hours, then dehydrated with ethanol and embedded in Epon. With a dry diamond knife, 100-nm sections were cut perpendicular to the *c* axis of the crystals. The sections were transferred to a water surface with a fine hair and picked up immediately on copper grids to prevent dissolution of the crystals. Images and diffraction data were obtained with a Philips 200 electron microscope. Images were recorded at 60 kV and diffraction data at 100 kV.

The electron micrographs of *Mya arenaria* and *Spisula solidissima* (Fig. 1) show hinge ligament cross sections. The electron-opaque structures are the aragonite crystals; the electron lucent area is the organic matrix. Since the *c* axes of the individual crystals (which are nearly perpendicular to the plane of the micrographs) are not perfectly parallel, not all of the crystals in a section are in a reflecting orientation. Those crystals that are in a strongly reflecting orientation have opaque images as a result of

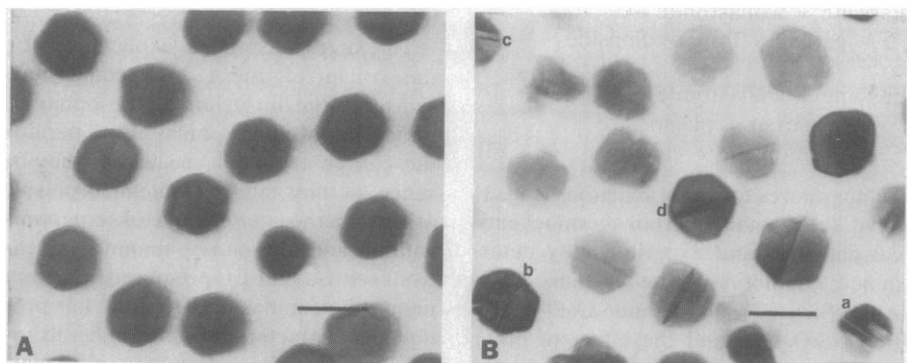


Fig. 1. Electron micrographs of hinge ligaments showing the aragonite crystals in cross section. (A) The *Mya arenaria* ligament. The thin bands through the center of the crystals are thin twin lamellae. (B) The *Spisula solidissima* ligament. Crystal *a* has multiple twin lamellae and crystal *b* has twin lamellae on both the (110) and (1 $\bar{1}$ 0) planes. Crystal *c* has a thick twin lamella and the lower third of crystal *a* is in the twin orientation. Bar equals 100 nm.

the interception of the diffracted beam by the objective aperture; the weakly reflecting crystals have light images.

The crystals in the *Mya* ligament (Fig. 1A) have a thin band through the center of the crystal because of diffraction contrast from a thin twin lamella on the (110) plane (5). The two halves of the parent crystal are in the same orientation; the thin lamella is in twin orientation (that is, rotated 63.8° about the *c* axis) with respect to the parent. Since the twin lamella of all the crystals have nearly the same orientation, the crystals are well aligned with respect to rotation about the *c* axis, and, since the crystal images are of nearly uniform intensity, the *c* axis of the crystals is nearly parallel as well. This is not the case in the *Spisula* ligament (Fig. 1B). Here the crystals appear to have a nearly random orientation about the *c* axis, and the variation in intensity demonstrates the nonparallel alignment of the *c* axes. The twinning pattern is also very irregular. In addition to the thin twin through the center of the crystal, there is often a series of twin lamellae (crystal *a* in Fig. 1B) or twin lamellae on both the (110) and ( $\bar{1}\bar{1}0$ ) planes (crystal *b* in Fig. 1B). Some crystals have a large component in the twin orientation. Crystal *c* (Fig. 1B) has a thick twin lamella, and the lower third of crystal *a* (Fig. 1B) is in the twin orientation.

To confirm the crystal twinning, electron diffraction images were obtained of individual crystals by using a selective area aperture. Selected crystals had the *c* axis oriented parallel with the electron beam in order to generate the *hk0* reciprocal lattice net (Fig. 2). Figure 2C is a diagram of the predicted *hk0* net for twinned aragonite and has the same orientation as the diffraction images. The black circles represent the parent reflections and the open circles the twin reflections, which are coincident for reflections (*hh0*). The line segments in the diagram represent double diffraction of parent reflections by the twin and twin reflections by the parent. Theoretically, an indefinite number of these reflections can occur along the [110] zone axes, but in practice only a few are observed since the intensity of the diffracted beam decreases for higher order reflections. Electron diffraction patterns of twinned crystals have been described (5).

Figure 2A is a diffraction pattern from a crystal which has a large component in the twin orientation such as crystal *a* or *c* (Fig. 1B). This reciprocal lattice net can be indexed by reference to the diagram and crystallographic data in Fig. 2C. Figure 2B is a diffraction pattern from a

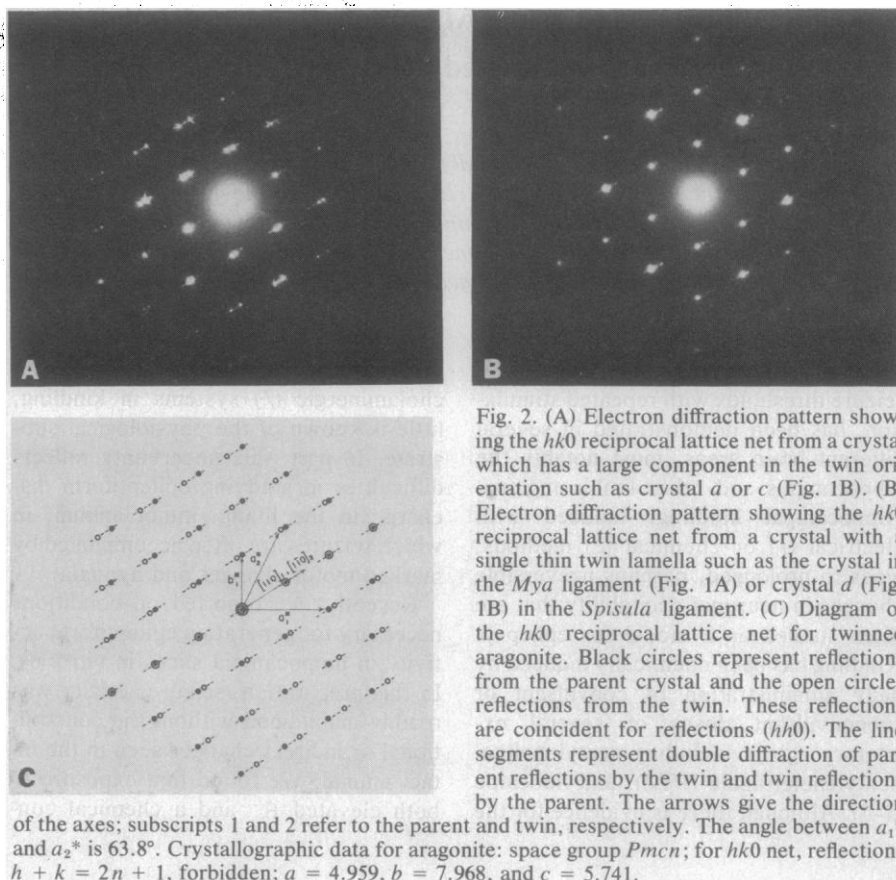


Fig. 2. (A) Electron diffraction pattern showing the *hk0* reciprocal lattice net from a crystal which has a large component in the twin orientation such as crystal *a* or *c* (Fig. 1B). (B) Electron diffraction pattern showing the *hk0* reciprocal lattice net from a crystal with a single thin twin lamella such as the crystal in the *Mya* ligament (Fig. 1A) or crystal *d* (Fig. 1B) in the *Spisula* ligament. (C) Diagram of the *hk0* reciprocal lattice net for twinned aragonite. Black circles represent reflections from the parent crystal and the open circles reflections from the twin. These reflections are coincident for reflections (*hh0*). The line segments represent double diffraction of parent reflections by the twin and twin reflections by the parent. The arrows give the direction of the axes; subscripts 1 and 2 refer to the parent and twin, respectively. The angle between  $a_1^*$  and  $a_2^*$  is 63.8°. Crystallographic data for aragonite: space group *Pm $\bar{c}n$* ; for *hk0* net, reflections  $h + k = 2n + 1$ , forbidden;  $a = 4.959$ ,  $b = 7.968$ , and  $c = 5.741$ .

crystal with a single thin twin lamella such as the crystals in the *Mya* ligament (Fig. 1A) or crystal *d* (Fig. 1B) in the *Spisula* ligament. In this case, the twin primary reflection intensities are no stronger than many of the double diffraction reflections, because the twin lamella is very thin (less than 5 nm) compared to the crystal diameter (about 100 nm) and crystal thickness (about 100 nm), making it improbable for a twin primary diffraction beam to emerge from the crystal before a secondary diffraction by the parent crystal has occurred. The reflections in the diffraction pattern tend to have a star-shaped, instead of circular, structure. This is due to diffraction artifacts caused by irregularities in the circular selective area aperture.

Crystal twinning is always apparent in thin sections irrespective of the angle used between the (110) twinning plane of the crystals and the knife-edge during section preparation. The distribution of twin structures within the ligament crystals differs with species, as was demonstrated with *Mya arenaria* and *Spisula solidissima*. Cahn (6) has stated that, although aragonite undergoes mechanical twinning by shear when heated, it never twins through mechanical stressing alone. It is, therefore, unlikely that the ligament crystals were mechanically twinned during processing for electron

microscopy but were twinned during growth in situ.

Rapid precipitation and the presence of foreign substances favor twinning in many crystals. It has been proposed that the ionic constituents of tissue fluids or the structure and composition of the organic matrix or matrix vesicles are responsible for the nucleation, growth, orientation, and polymorphic form of biogenic calcium crystals (7). Twinning in biological mineral deposits is probably influenced by these same factors.

MARY E. MARSH, RONALD L. SASS  
Department of Biology, Rice  
University, Houston, Texas 77001

#### References and Notes

1. W. L. Bragg, *Proc. R. Soc. London Ser. A* **105**, 16 (1924).
2. B. J. Burridge and D. R. Pirkethly, *Phys. Status Solidi* **32**, 399 (1969).
3. H. Mutvei, *Calcif. Tissue Res.* **24**, 11 (1977).
4. M. Marsh, G. Hopkins, F. Fisher, R. Sass, *J. Ultrastruct. Res.* **54**, 445 (1976); G. Bevelander and H. Nakahara, *Calcif. Tissue Res.* **4**, 101 (1969).
5. P. B. Hirsch, A. Howie, R. B. Nicholson, D. W. Pashley, M. J. Whelan, *Electron Microscopy of Thin Crystals* (Butterworths, Washington, D.C., 1965), pp. 141-152.
6. R. W. Cahn, *Adv. Phys.* **3**, 363 (1954).
7. M. J. Glimcher, in *Calcification in Biological Systems*, R. F. Sogannes, Ed. (AAAS, Washington, D.C., 1960), p. 421; K. M. Wilbur, in *Physiology of Mollusca*, K. M. Wilbur and C. M. Yonge, Eds. (Academic Press, New York, 1964), vol. 1, p. 243; H. C. Anderson, *J. Cell Biol.* **41**, 59 (1969); E. Bonucci, *Z. Zellforsch. Mikrosk. Anat.* **103**, 192 (1970).
8. Supported by NIH grants AM-18582 and DE-00078.

3 December 1979; revised 5 February 1980